

## RESEARCH ARTICLE

# A High-Performance Microstrip Triplexer With Compact Size, Flat Channels and Low Losses for 5G Applications

**SALAH I. YAHYA**<sup>1,2</sup>, (Senior Member, IEEE), **FARID ZUBIR**<sup>3</sup>, (Member, IEEE),  
**LEILA NOURI**<sup>4,5</sup>, **ABBAS REZAEI**<sup>6</sup>, **FAWWAZ HAZZAZI**<sup>7</sup>,  
**MUHAMMAD AKMAL CHAUDHARY**<sup>8</sup>, (Senior Member, IEEE), **MAHER ASSAAD**<sup>9</sup>,  
**ZUBAIDA YUSOFF**<sup>9</sup>, (Senior Member, IEEE), AND **BINH NGUYEN LE**<sup>4,5</sup>

<sup>1</sup>Department of Communication and Computer Engineering, Cihan University-Erbil, Erbil 44001, Iraq

<sup>2</sup>Department of Software Engineering, Faculty of Engineering, Koya University, Koya KOY45, Iraq

<sup>3</sup>Wireless Communication Centre, Faculty of Electrical Engineering, Universiti Teknologi Malaysia, Johor Bahru, 81310 Johor, Malaysia

<sup>4</sup>Institute of Research and Development, Duy Tan University, Da Nang 50000, Vietnam

<sup>5</sup>School of Engineering & Technology, Duy Tan University, Da Nang 50000, Vietnam

<sup>6</sup>Department of Electrical Engineering, Kermanshah University of Technology, Kermanshah 6715685420, Iran

<sup>7</sup>Department of Electrical Engineering, College of Engineering in Al-Kharj, Prince Sattam bin Abdulaziz University, AlKharj 11492, Saudi Arabia

<sup>8</sup>Department of Electrical and Computer Engineering, College of Engineering and Information Technology, Ajman University, United Arab Emirates

<sup>9</sup>Faculty of Engineering, Multimedia University, Persiaran Multimedia, Cyberjaya, 63100 Selangor, Malaysia

Corresponding authors: Leila Nouri (leilanouri@duytan.edu.vn), Farid Zubir (faridzubir@utm.my), and Zubaida Yusoff (zubaida@mmu.edu.my)

This work was supported in part by the Higher Institution Centre of Excellence (HICOE), Ministry of Higher Education Malaysia through the Wireless Communication Centre (WCC), Universiti Teknologi Malaysia, under Grant R.J090301.7823.4J610; in part by Universiti Teknologi Malaysia (UTM) under UTM Encouragement Research under Grant 20J65; in part by UTMShine Batch 6 under Grant 09G97; and in part by the Faculty of Engineering, Multimedia University, Cyberjaya (MMU).

**ABSTRACT** A new microstrip triplexer with a compact size of  $0.007 \lambda_g^2$  is proposed in this work, where designing a microstrip triplexer with a size less than  $0.01 \lambda_g^2$  is a big challenge. In addition to the compact size, it shows a high performance i.e. its channels are wide with low insertion losses. Moreover, the channels are flat with three low group delays (GDs) of 0.65, 0.95 and 1.17 ns, while most of the previously reported triplexers have not considered this important parameter. The proposed resonator is mathematically analyzed to find a method to get rid of harmonics and tune the resonance frequency. Meanwhile, the 1<sup>st</sup>, 2<sup>nd</sup>, 3<sup>rd</sup> and 4<sup>th</sup> harmonics are suppressed above the first channel. The designed triplexer is suitable for 5G mid-band applications. The proposed triplexer is exactly fabricated and then measured to confirm the designing method and simulation results. The obtained results show that all the simulation, mathematical analysis and experimental results are in good agreement. Therefore, the proposed triplexer can be easily used in designing high-performance RF communication systems.

**INDEX TERMS** Microstrip, compact, triplexer, harmonic, 5G, group delay.

## I. INTRODUCTION

High-performance microstrip filtering devices such as couplers, diplexers and triplexers have been extensively applied in wireless RF communication applications [1], [2], [3], [4], [5], [6], [7], [8]. In [8], [9], [10], [11], [12], [13], [14],

The associate editor coordinating the review of this manuscript and approving it for publication was Yogendra Kumar Prajapati<sup>10</sup>.

[15], [16], [17], [18], [19], [20], [21], [22], [23], and [24], various types of microstrip planar resonators and triplexers are reported and all of them occupy large implementation areas greater than  $0.01 \lambda_g^2$ . Coupled open-loops [8], [9], coupled lines [10], coupled hairpin resonators [11], stub-loaded coupled open-loops [12] and coupled U-shapes [13] are some examples of using the coupling structure in designing microstrip components. Also, various mathematical analysis

techniques have been employed in the design of microstrip triplexers such as: even and odd mode analysis [5], mathematical analysis of step impedance resonators (SIR) [6], determination of lumped element values for a proposed microstrip structure [7], presentation of coupling matrices [8], calculation of input impedance for a three-channel filter [10] and obtaining Z-parameters for a presented resonator [13]. In [14], a triple-mode microstrip resonator is used to design a narrow-channel triplexer with high insertion losses. To design of a microstrip triplexer working at 1 GHz, 1.25 GHz and 1.5 GHz, coupled hairpin resonators are integrated in [15]. The introduced triplexer in [16] works at 2.67 GHz (4G LTE), 3.43 GHz and 3.1 GHz (IEEE802.16 WiMAX). In [17], a microstrip triplexer with coupled zigzag lines is introduced for WLAN and GSM applications. Open-loops are used to design a microstrip diplexer and a microstrip triplexer in [18]. Similar to [15], microstrip coupled hairpin resonators are used to design a triplexer in [19]. But this microstrip triplexer occupies a very large implementation area of  $0.119 \lambda_g^2$ . Another common problem of the proposed triplexers in [18], [19], [20], and [21] is having large insertion losses. A microstrip channel-continuous triplexer with high insertion losses and several transmission zeroes is presented in [22]. Coupled loops with internal coupled lines are used to achieve a microstrip triplexer in [23]. An important factor of a well-designed passive filtering device is having low group delay (GD). Because the group delay is a type of distortion that can change the shape of a signal. Despite this fact, none of the previous triplexers tried to decrease group delays significantly. Therefore, as a general result it can be said that most of the previous triplexers have large dimensions and high losses. Moreover, none of the previous designs has made any efforts to improve the group delays significantly. Accordingly, we will try to solve these problems by introducing a new structure. Our aim is to obtain a new microstrip triplexer with low losses, low group delays, flat channels and a very compact size that can be easily used in designing high-performance RF communication systems. We will present a perfect mathematical design method to analyze a new proposed resonator. This method includes calculating the ABCD matrix and extracting the scattering parameters. Then, three bandpass filters (BPFs) will be designed based on the analyzed resonator. By integrating these filters, a new microstrip triplexer for 5G mid-band applications will be obtained.

**II. DESIGN OF PROPOSED TRIPLEXER**

To obtain a microstrip triplexer, we need to design a new microstrip resonator. Our proposed resonator is a stub-loaded line coupled to a transmission line. Fig. 1 shows our resonator, its approximated LC circuit and its simplified LC circuit. The open ends of the coupled lines are presented by the capacitors  $C_0$ . The equivalent of the coupling effect is approximated by a small capacitor of  $C$ , which is usually in the fF range. The lines indicated by the lengths  $l_a$  and  $l_b$  are replaced by the

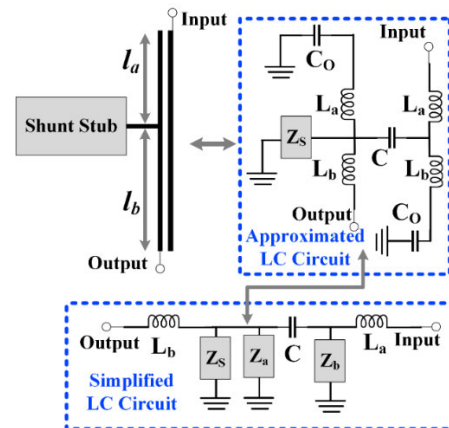


**FIGURE 1.** Proposed new resonator with its approximated LC circuits.

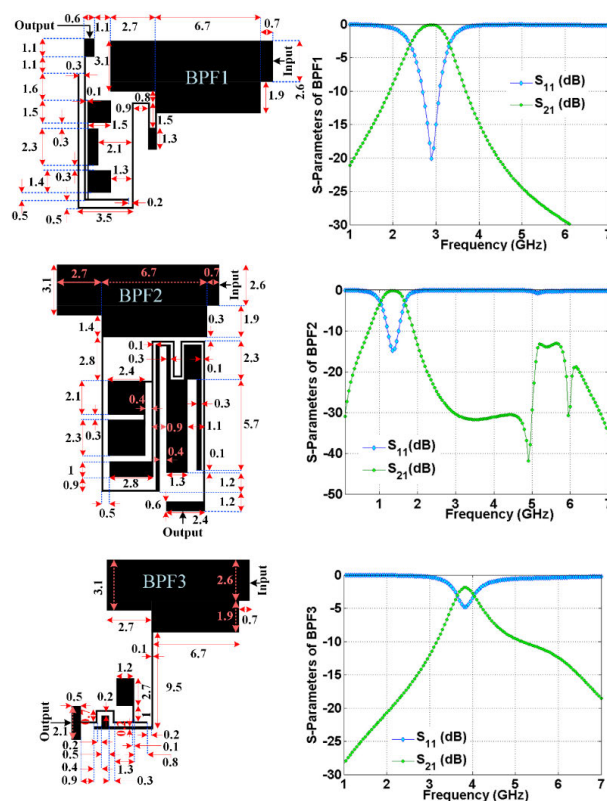


**FIGURE 2.** Proposed BPFs: layouts and frequency responses (Unit: mm and all the thinnest lines have widths of 0.1 mm).

inductors  $L_a$  and  $L_b$  respectively. Also, the impedance of the shunt stub is shown by  $Z_s$ .

In the simplified LC circuit, the impedances  $Z_a$  and  $Z_b$  are given by:

$$Z_a = j\omega L_a + \frac{1}{j\omega C_0}$$

$$Z_b = j\omega L_b + \frac{1}{j\omega C_0} \tag{1}$$

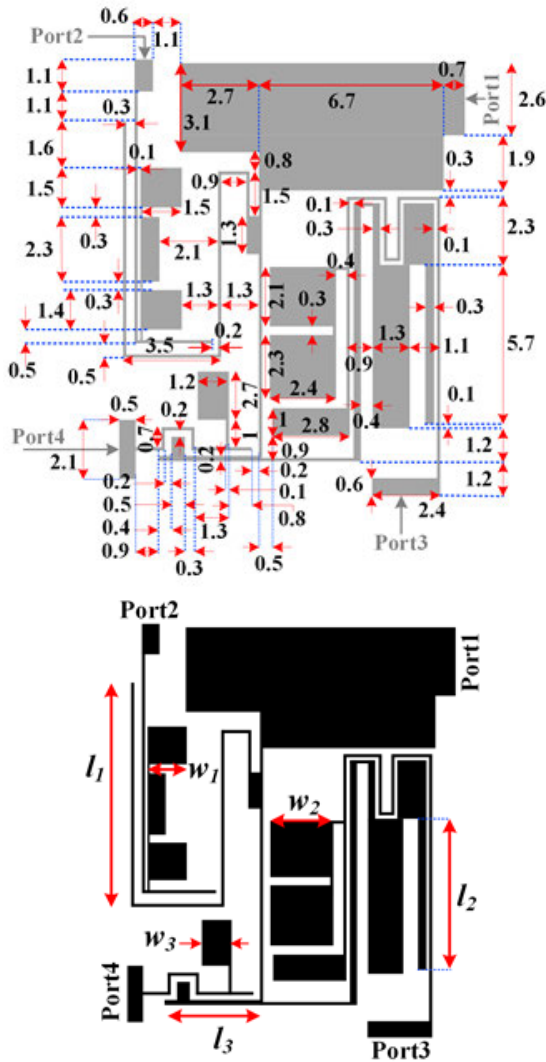


FIGURE 3. The layout of the proposed triplexer (unit: mm).

The ABCD matrix from the input port to the output port (T) can be written as:

$$\begin{aligned}
 T &= \begin{bmatrix} A & B \\ C & D \end{bmatrix} = \begin{bmatrix} 1 & j\omega L_a \\ 0 & 1 \end{bmatrix} \times \begin{bmatrix} 1 & 0 \\ \frac{1}{Z_b} & 1 \end{bmatrix} \times \begin{bmatrix} 1 & \frac{1}{j\omega C} \\ 0 & 1 \end{bmatrix} \\
 &\times \begin{bmatrix} 1 & \frac{1}{Z_s} + \frac{1}{Z_a} & 0 \\ \frac{1}{Z_s} + \frac{1}{Z_a} & 1 & 1 \end{bmatrix} \times \begin{bmatrix} 1 & j\omega L_b \\ 0 & 1 \end{bmatrix} \rightarrow \\
 A &= 1 + \frac{j\omega L_a}{Z_b} + \left(\frac{1}{j\omega C} + \frac{L_a}{CZ_b} + j\omega L_a\right) \left(\frac{1}{Z_s} + \frac{1}{Z_a}\right) \\
 B &= \frac{1}{j\omega C} + \frac{L_a}{CZ_b} + j\omega L_a + j\omega L_b \left[1 + \frac{j\omega L_a}{Z_b} \right. \\
 &\quad \left. + \left(\frac{1}{j\omega C} + \frac{L_a}{CZ_b} + j\omega L_a\right) \left(\frac{1}{Z_s} + \frac{1}{Z_a}\right)\right] \\
 C &= \frac{1}{Z_b} + \frac{1}{Z_s} + \frac{1}{Z_a} + \frac{1}{j\omega CZ_b Z_s} + \frac{1}{j\omega CZ_b Z_a} \\
 D &= j\omega L_b \left[\frac{1}{Z_b} + \left(1 + \frac{1}{j\omega CZ_b}\right) \left(\frac{1}{Z_s} + \frac{1}{Z_a}\right)\right] + \left(1 + \frac{1}{j\omega CZ_b}\right)
 \end{aligned} \tag{2}$$

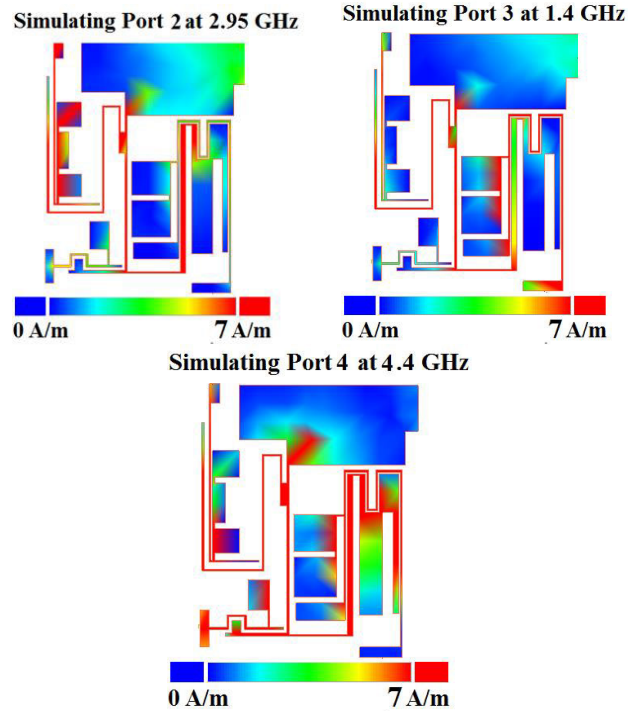


FIGURE 4. Current density distribution of the designed triplexer.

By substituting (1) in (2), the following equations can be obtained:

$$\begin{aligned}
 A &= 1 + \frac{j\omega L_a}{j\omega L_b + \frac{1}{j\omega C_0}} \\
 &\quad + \left(\frac{1}{j\omega C} + \frac{L_a}{C(j\omega L_b + \frac{1}{j\omega C_0})} + j\omega L_a\right) \\
 &\quad \times \left(\frac{1}{Z_s} + \frac{1}{j\omega L_a + \frac{1}{j\omega C_0}}\right) \\
 B &= \frac{1}{j\omega C} + \frac{L_a}{C(j\omega L_b + \frac{1}{j\omega C_0})} + j\omega L_a \\
 &\quad + j\omega L_b \left[1 + \frac{j\omega L_a}{j\omega L_b + \frac{1}{j\omega C_0}} + \left(\frac{1}{j\omega C} + \frac{L_a}{C(j\omega L_b + \frac{1}{j\omega C_0})} \right. \right. \\
 &\quad \left. \left. + j\omega L_a\right) \left(\frac{1}{Z_s} + \frac{1}{j\omega L_a + \frac{1}{j\omega C_0}}\right)\right] \\
 C &= \frac{1}{j\omega L_b + \frac{1}{j\omega C_0}} + \frac{1}{Z_s} + \frac{1}{j\omega L_a + \frac{1}{j\omega C_0}} \\
 &\quad + \frac{1}{j\omega C(j\omega L_b + \frac{1}{j\omega C_0})Z_s} \\
 &\quad + \frac{1}{j\omega C(j\omega L_b + \frac{1}{j\omega C_0})(j\omega L_a + \frac{1}{j\omega C_0})} \\
 D &= j\omega L_b \left[\frac{1}{j\omega L_b + \frac{1}{j\omega C_0}} + \left(1 + \frac{1}{j\omega C(j\omega L_b + \frac{1}{j\omega C_0})} \right. \right. \\
 &\quad \left. \left. \times \left(\frac{1}{Z_s} + \frac{1}{j\omega L_a + \frac{1}{j\omega C_0}}\right)\right)\right]
 \end{aligned}$$

$$+ 1 + \frac{1}{j\omega C(j\omega L_b + \frac{1}{j\omega C_0})} \quad (3)$$

If we select the shunt stub as a low-impedance section, then:

$$\begin{aligned} \frac{1}{Z_S} + \frac{1}{j\omega L_a + \frac{1}{j\omega C_0}} &\approx \frac{1}{Z_S} \\ \frac{1}{Z_S} + \frac{1}{j\omega L_a + \frac{1}{j\omega C_0}} &\approx \frac{1}{Z_S} \\ \frac{1}{j\omega L_b + \frac{1}{j\omega C_0}} + \frac{1}{Z_S} + \frac{1}{j\omega L_a + \frac{1}{j\omega C_0}} &\approx \frac{1}{Z_S} \end{aligned} \quad (4)$$

As mentioned before, C is a small capacitor in the fF range. On the other hand,  $\omega$  is our predetermined angular frequency which is in the GHz range. For achieving this frequency, we have to choose the values of inductors in the nH range. Therefore, we can use other approximations as follows:

$$\begin{aligned} \frac{1}{j\omega C} + \frac{L_a}{C(j\omega L_b + \frac{1}{j\omega C_0})} + j\omega L_a \\ \approx \frac{1}{j\omega C} + \frac{L_a}{C(j\omega L_b + \frac{1}{j\omega C_0})} \\ = \frac{1}{j\omega C} (1 + \frac{L_a}{L_b - \frac{1}{\omega^2 C_0}}) \\ \times \frac{1}{j\omega C(j\omega L_b + \frac{1}{j\omega C_0})Z_S} \\ \gg \frac{1}{j\omega C(j\omega L_b + \frac{1}{j\omega C_0})(j\omega L_a + \frac{1}{j\omega C_0})} \\ + \frac{1}{j\omega L_b + \frac{1}{j\omega C_0}} + \frac{1}{Z_S} + \frac{1}{j\omega L_a + \frac{1}{j\omega C_0}} \end{aligned} \quad (5)$$

By applying the above approximations and also by using (4) and (5), (3) can be summarized as follows:

$$\begin{aligned} A &\approx \frac{1}{j\omega CZ_S} + \frac{L_a}{CZ_S(j\omega L_b + \frac{1}{j\omega C_0})} \\ B &\approx \frac{L_b}{CZ_S} + \frac{L_a L_b \omega}{CZ_S(\omega L_b - \frac{1}{\omega C_0})} \\ C &\approx \frac{1}{j\omega C(j\omega L_b + \frac{1}{j\omega C_0})Z_S} \\ D &\approx \frac{L_b}{CZ_S(j\omega L_b + \frac{1}{j\omega C_0})} \end{aligned} \quad (6)$$

Using the ABCD parameters, we can extract the scattering parameter  $S_{21}$  as follows [24]:

$$S_{21} = \frac{2CZ_S}{\frac{1}{j\omega} + \frac{2L_a}{(j\omega L_b + \frac{1}{j\omega C_0})} + \frac{L_b}{Z_0} + \frac{L_a L_b \omega}{Z_0(\omega L_b - \frac{1}{\omega C_0})} + \frac{Z_0}{\frac{1}{C_0} - \omega^2 L_b}} \quad (7)$$

As mentioned before,  $Z_S$  should have a low impedance and C has a very small value. Therefore,  $CZ_S$  has a small value near zero. To have a low insertion loss near zero,  $|S_{21}|$  should

be near 1. Therefore, the real and imaginary parts of the denominator of  $S_{21}$  should be zero. Accordingly, we can extract the conditions to have a low insertion loss as follows:

$$\begin{aligned} \frac{1}{j\omega} + \frac{2L_a}{(j\omega L_b + \frac{1}{j\omega C_0})} &\approx 0 \rightarrow \omega_{r1} \\ &\approx \frac{1}{\sqrt{(2L_a + L_b)C_0}} \\ \frac{L_b}{Z_0} + \frac{L_a L_b \omega}{Z_0(\omega L_b - \frac{1}{\omega C_0})} + \frac{Z_0}{\frac{1}{C_0} - \omega^2 L_b} &\approx 0 \rightarrow \omega_{r2} \\ &\approx \sqrt{\frac{L_b + Z_0^2 C_0}{L_b C_0(L_a + L_b)}} \end{aligned} \quad (8)$$

Therefore, at the angular resonance frequencies  $\omega_{r1}$  and  $\omega_{r2}$ , the insertion losses can have the minimum values. According to (8) and for a predetermined angular resonance frequency, by increasing the coupling capacitor we can reduce the inductors  $L_a$  and  $L_b$ . Subsequently, reducing these inductors makes the physical length of the transmission line ( $l_a$  and/or  $l_b$ ) shorter. To increase the coupling capacitor, the space between coupled lines can be reduced. But our aim is designing a resonator with only one resonance frequency, so  $\omega_{r1}$  or  $\omega_{r2}$  acts as a harmonic that must be eliminated. One way to eliminate this harmonic is to set both angular frequencies equal to each other. Based on this method, it can be written that:

$$\begin{aligned} \frac{1}{(2L_a + L_b)C_0} = \frac{L_b + Z_0^2 C_0}{L_b C_0(L_a + L_b)} \rightarrow L_a L_b \\ + 2L_a Z_0^2 C_0 + Z_0^2 C_0 L_b = 0 \end{aligned} \quad (9)$$

Due to the positive values of the inductors and capacitors, it is impossible to reach (9). So another method to eliminate the harmonic is putting it at high frequencies. To achieve this goal, the following equation can be used:

$$\begin{aligned} \frac{1}{(2L_a + L_b)C_0} \ll \frac{L_b + Z_0^2 C_0}{L_b C_0(L_a + L_b)} \rightarrow L_a L_b \\ + 2L_a Z_0^2 C_0 + Z_0^2 C_0 L_b \gg 0 \end{aligned} \quad (10)$$

According to the last equation, a high degree of freedom exists for shifting the harmonics to high frequencies. Therefore, our resonator is suitable to design of a triplexer. However, at first we designed three BPFs named BPF1, BPF2 and BPF3 using the analyzed stub-loaded coupled lines. These filters and their frequency responses are shown in Fig.2.

Since the input port will be common in the final triplexer layout, we didn't change its dimensions for all of the BPFs. The BPFs are simulated by ADS software using its EM simulator. A Rogers RT/duroid 5880 substrate with 31 mil thickness,  $\epsilon_r = 2.22$  and 0.0009 loss tangent is used to simulate our filters. BPF1 has a 20 dB return loss and 0.08 dB insertion loss. It works at 2.95 GHz. The insertion loss of BPF3 at 1.4 GHz is 0.18 dB. The proposed BPFs are designed to be easily connected to each other. In BPF3, the length of coupled lines is short, which leads to a high insertion loss of

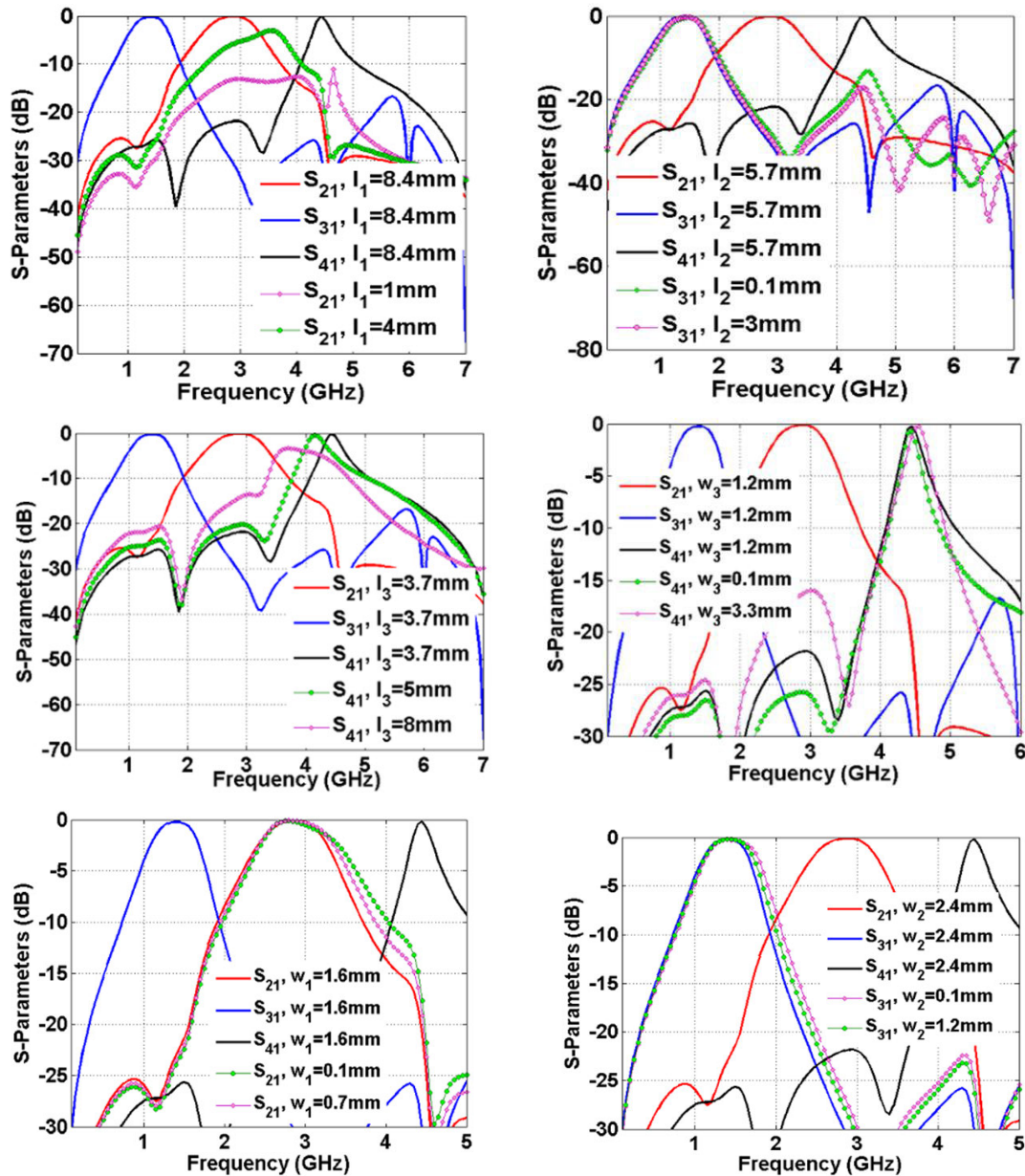


FIGURE 5. Frequency responses as functions of the significant physical dimensions.

1.8 dB at 3.85 GHz. However, after connecting to other filters this factor can be improved.

By integrating the designed BPFs, the proposed microstrip triplexer is obtained as presented in Fig.3. As shown in this figure, we didn't change the dimensions of the designed BPFs. The size of our introduced triplexer is  $15.5\text{mm} \times 12.3\text{mm} = 0.094\lambda_g \times 0.074\lambda_g$ . We calculated  $\lambda_g$  (the guided wavelength) at 1.4 GHz.

To optimize the triplexer structure, we changed the significant lengths and widths presented in Fig.3 ( $l_1$ ,  $l_2$ ,  $l_3$ ,  $w_1$ ,  $w_2$  and  $w_3$ ). We selected them based on the results of the mathematical analysis of the proposed resonator and also the distribution of current density shown in Fig.4.

Fig.4 depicts the distribution of the current density of the designed triplexer for simulating port 2 (at 2.95 GHz), port 3 (at 1.4 GHz) and port 4 (at 4.4 GHz). As shown in Fig.4, the thin lines have high current densities. Therefore, tuning these lines is significant to improve the frequency response. As can be seen, by simulating port 2 at 2.95 GHz, the thin stub near this port shows high current density distribution. For port 3 at 1.4 GHz, the thin line connected to this port has a high current density. Accordingly, to improve the performance of the first channel we can change the dimensions of this physical length ( $l_2$  in Fig.3). For simulating port 4, the loading effects of the other filters can be further investigated which can help to improve the performance of the last channel.

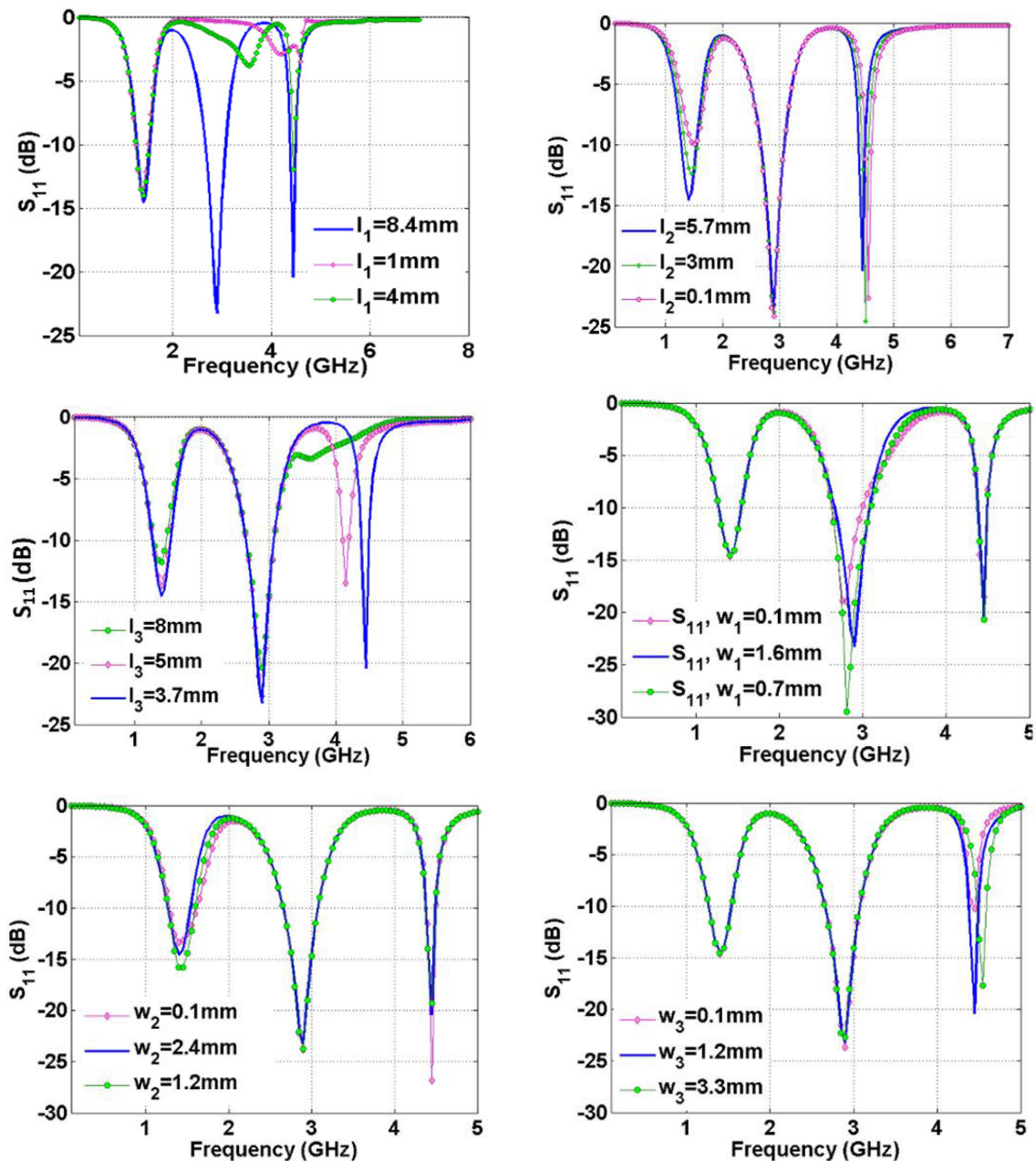


FIGURE 6.  $S_{11}$  as functions of the significant physical dimensions.

Fig.5 shows the frequency responses as function of the physical dimensions ( $w_1$ ,  $w_2$ ,  $l_1$ ,  $l_2$ ,  $w_3$  and  $l_3$ ). The results show that the middle, lower and upper channels are significantly affected by the lengths  $l_1$ ,  $l_2$  and  $l_3$  respectively. By decreasing the length  $l_1$ , the middle channel will be broken. Reducing  $l_2$  increases the level of harmonics. This is because, to remove the harmonic the length of the coupled lines must be increased. This issue is already proved theoretically and also confirmed in (10). Changing the widths has less effect on the frequency response than changing the lengths. This issue is verified by the current density distribution curves. Increasing  $w_1$  and  $w_2$  moves the 2<sup>nd</sup> and 1<sup>st</sup> channels to the left, which can help in miniaturization.

However, increasing  $l_3$  improves the selectivity of the last channel.

Fig.6 illustrates  $S_{11}$  as functions of these significant physical dimensions. The results show that decreasing  $l_1$  and  $l_2$  leads to an increase in the return loss. Meanwhile, decreasing  $w_2$  improves return loss in the last channel which is due to having a positive loading effect of the BPFs. Increasing  $l_3$ , destroys  $S_{11}$  in the last band. As can be seen,  $l_3 = 3.7$  mm is the best choice to improve the return loss.

### III. RESULTS AND DISCUSSIONS

We simulated and measured the designed microstrip triplexer using the EM simulator of ADS software and an HP8757A

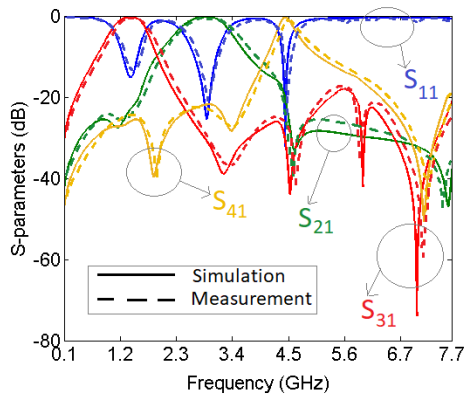


FIGURE 7. Transition parameters (simulated and measured).

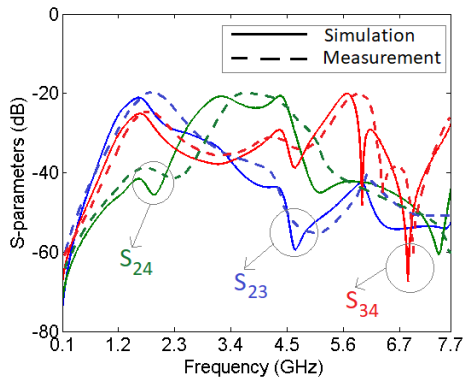


FIGURE 8. Isolations between the output ports (simulated and measured).

network analyzer, respectively. HP8757A network analyzer has the following features:

- Frequency ranges: 10 MHz-60 GHz
- Accurate swept power measurements (dBm)
- 40 dB directivity bridges
- Four input ports
- Four independent display channels
- Direct plotter or printer output

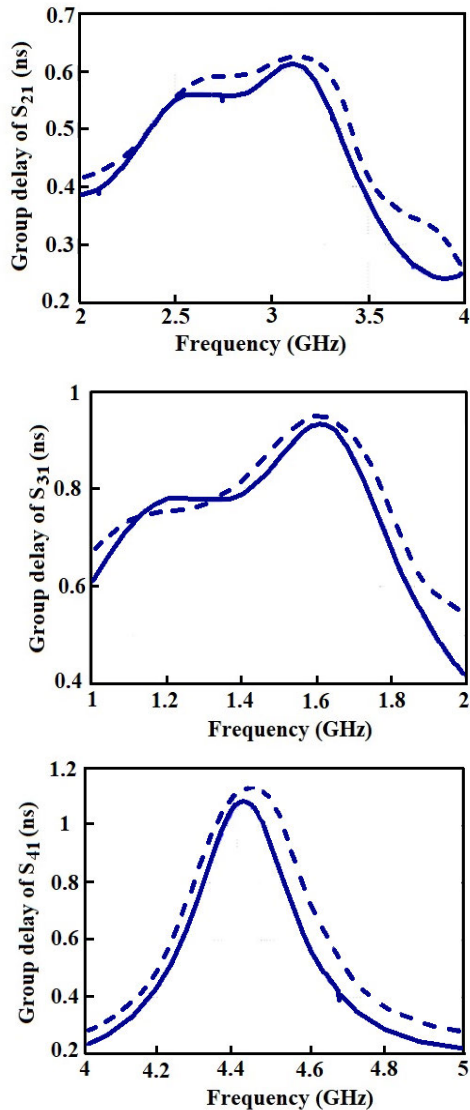
The substrate of the fabricated microstrip triplexer is RT/duroid 5880 ( $h=0.7874$  mm,  $\epsilon_r = 2.22$  and  $\tan(\delta) = 0.0009$ ). The obtained measurement and simulation results of the transition parameters are depicted in Fig.7. The resonance frequencies are 1.4 GHz, 2.9 GHz and 4.4 GHz. The return losses and insertion losses are (15 dB and 0.19 dB) for the lower band, (25.2 dB and 0.08 dB) for the middle band and (32 dB and 0.19 dB) for the upper band. Since there are SMA and copper losses, the losses obtained by the simulations are smaller than the measurements. As can be seen, the channels are wide and flat, where the fractional bandwidths (FBW%) of the 1<sup>st</sup>, 2<sup>nd</sup> and 3<sup>rd</sup> channels are 49%, 34% and 7.2% respectively. The maximum harmonic level from DC up to 7.7 GHz is lower than  $-18$  dB. There are several transition zeros at the stopband of all channels. Therefore, after the first channel, the 1<sup>st</sup> to 4<sup>th</sup> harmonics are suppressed. Fig.8 presents the obtained measured and simulated isolation between the output ports. The maximum levels of  $S_{23}$ ,  $S_{24}$  and  $S_{34}$  are below  $-19$  dB.

TABLE 1. Comparison in terms of resonance frequencies ( $F_{R1}$ ,  $F_{R2}$ ,  $F_{R3}$ ), insertion losses ( $IL_1$ ,  $IL_2$ ,  $IL_3$ ), return losses ( $RL_1$ ,  $RL_2$ ,  $RL_3$ ), fractional bandwidths ( $\Delta_1$ ,  $\Delta_2$ ,  $\Delta_3$ ) and sizes (\*: approximated values).

Refs	$f_{r1}, f_{r2}, f_{r3}$ (GHz)	$IL_1, IL_2, IL_3$ (dB)	$RL_1, RL_2, RL_3$ (dB)	$\Delta_1, \Delta_2, \Delta_3$	Size ( $\lambda_g^2$ )
This Triplexer	1.4, 2.9, 4.4	0.19, 0.08, 0.19	15, 25.2, 32	49%, 34%, 7.2%	0.007
[5]	3.2, 3.7, 4.4	2.7, 2.5, 1.8	16, 16, 16	6.5%, 7%, 8%	0.048
[6]	1.4, 1.7, 1.9	3.4, 3.5, 3.6	---	4.96%, 4.57%, 4.82%	0.358
[7]	1.2, 1.8, 2.4	1.3, 1.3, 1.2	11.6, 14, 10	14.4%, 14%, 13.6%	0.055
[8]	3.3, 3.89, 4.56	2.2, 2.3, 2.3	Better than 14	---	0.275
[9]	0.9, 2.45, 5.35	0.37, 0.68, 0.4	11.8, 21.3, 13.8	---	0.088
[10]	1.5, 1.7, 1.9	4.9, 5.8, 5.95	---	3.3%, 2.9%, 3.6%	0.132
[11]	1.88, 2.1, 2.6	1.3, 2.3, 3.2	22, 25, 21	0.86%, 1.4%, 0.96%	0.1*
[12]	1, 1.25, 1.5	2.7, 1.8, 3.2	Better than 16	9.5%, 4.2%, 4.5%	0.064
[13]	2.67, 3.1, 3.43	0.72, 0.63, 0.71	24.5, 24, 24.7	---	0.137
[14]	1.4, 1.8, 3.2	0.1, 2, 1	25, 20, 20	5.2%, 2.8%, 9.4%	0.014
[15]	1.8, 3.2, 4.4	1.97, 1.99, 2.3	24, 22, 25	7.44%, 7.45%, 6.2%	0.177
[16]	2.4, 3.5, 5.8	0.9, 1.1, 1.3	---	6%, 4.5%, 3.6%	0.119
[17]	1.75, 2.35, 3.68	1.3, 1.4, 1.7	20, 25, 30	5.7%, 8.5%, 6.8%	0.027
[18]	1.45, 2.15, 2.75	3.6, 4.3, 4.8	15, 20, 15	6%, 6%, 4%	0.020
[19]	2.4, 3.5, 5.2	2.42, 1.62, 1.95	Better than 15	3%, 7%, 3%	0.164
[20]	2.3, 3.2, 3.6	0.78, 1.1, 0.62	19.8, 10, 28	5.2%, 5.5%, 1.6%	0.095
[21]	2.05, 2.45, 3.5	1.5, 1.8, 1.5	Better than 13	4.8%, 4%, 5.7%	0.346

To verify the advantages of this work, we compared it with the previous triplexers in Table 1. In this table, the indexes 1 to 3 are related to the 1<sup>st</sup> to 3<sup>rd</sup> bands respectively. As shown in Table 1, our triplexer occupies the minimum area ( $0.007 \lambda_g^2$ ) while we could not find a triplexer smaller than  $0.01 \lambda_g^2$ . Meanwhile, the best values of insertion loss (at all channels) and return loss (at the 2<sup>nd</sup> and 3<sup>rd</sup> channels) and the widest FBW (at the 1<sup>st</sup> and 2<sup>nd</sup> channels) are obtained in this work.

Another significant parameter in designing microstrip filtering devices is group delay, which is a type of distortion. It can change the shape of signals. Hence having a flat filtering passband with low group delay is an advantage. Despite



**FIGURE 9.** Simulated (solid lines) and measured (dashed lines) group delays of all channels.

this fact, most of the previous triplexers didn't pay attention to this issue. Because designing a triplexer is harder than diplexers and filters. The group delays of  $S_{21}$ ,  $S_{31}$  and  $S_{41}$  in their corresponding passbands are shown in Fig.9. As can be seen, the maximum simulated group delays at the lower, middle and upper channels are 0.62 ns, 0.93 ns and 1.15 ns respectively which are very good values for a triplexer. Also, the measured group delays are better than 1.2 ns at all channels.

We compared the measured group delays, types and the number of channels of our triplexer with the previous microstrip filtering devices in Table 2. As can be seen, compared to the previous works we could reduce this parameter significantly. Fig.10 illustrates a photograph of our triplexer. Compared to the previous works, we could obtain a triplexer with the most compact size, the minimum group delay and the lowest insertion losses. We used a new basic microstrip structure to obtain the proposed triplexer. Also, we used a

**TABLE 2.** Comparison in terms of group delays (GDS), type and the number of channels (NC).

Refs	NC	Type	Maximum GDS (ns)
This work	3	Triplexer	0.65, 0.95, 1.18
[25]	2	Diplexer	0.9, 1.1
[26]	4	Diplexer	2.76, 3.31, 0.91, 2.15
[27]	3	BPF	Better than 8ns at all channels
[28]	2	Diplexer	3, 3.14
[29]	3	BPF	3.67, 1.47, 0.83
[30]	2	Diplexer	3.15, 2.98
[31]	3	Triplexer	1.5, 6, 4.4
[32]	3	Triplexer	3, 3.1, 2.9



**FIGURE 10.** Fabricated triplexer.

new mathematical analysis to find a method to get rid of harmonics and tune the resonance frequency. All results of the mathematical analysis, simulation and measurement confirm each other. The applications of the proposed triplexer may vary depending on the region and regulatory requirements. This triplexer can be used in the following applications:

Wi-Fi and Bluetooth, weather and military radars, some satellite communication systems and scientific research applications such as spectroscopy, medical imaging and plasma physics.

#### IV. CONCLUSION

In this paper, a microstrip triplexer with a very compact size of  $0.007\lambda_g^2$ , flat channels, low group delays, low insertion losses (0.19/0.08/0.19 dB) and suppressed harmonics is designed, analyzed, fabricated and measured. It works at 1.4 GHz, 2.9 GHz and 4.4 GHz, which makes it suitable for 5G applications. The other advantage of this work is its wide channels, where the 1<sup>st</sup> and 2<sup>nd</sup> channels have the fractional bandwidths (FBW%) 49% and 34%, respectively. The proposed resonator is analyzed based on calculating the ABCD matrix and extracting  $S_{21}$ . To improve its performance, the designed triplexer is optimized. The comparison with the previous designs showed that our triplexer has the lowest insertion losses at all channels, the most compact size, the minimum group delays and the best return losses at the 2<sup>nd</sup> and 3<sup>rd</sup> channels.

#### REFERENCES

- [1] L. Nouri, S. I. Yahya, and A. Rezaei, "Design and fabrication of a compact branch-line hybrid coupler with a balanced phase using a new microstrip structure for GSM applications," *AEU-Int. J. Electron. Commun.*, vol. 161, Mar. 2023, Art. no. 154529.



- [2] A. Rezaei and S. I. Yahya, "A new design approach for a compact microstrip diplexer with good passband characteristics," *ARO-Sci. J. Koya Univ.*, vol. 10, no. 2, pp. 1–6, Aug. 2022.
- [3] K. Al-Majidi and Y. S. Mezaal, "New miniature narrow band microstrip diplexer for recent wireless communications," *Electronics*, vol. 12, no. 3, p. 716, Feb. 2023.
- [4] Y. Zhang, X. Tan, and Q. Xiang, "A compact frequency- and power-dividing ratio-tunable quadrature coupler," *Int. J. RF Microw. Comput.-Aided Eng.*, vol. 2023, pp. 1–8, Mar. 2023.
- [5] J.-Y. Wu, K.-W. Hsu, Y.-H. Tseng, and W.-H. Tu, "High-isolation microstrip triplexer using multiple-mode resonators," *IEEE Microw. Wireless Compon. Lett.*, vol. 22, no. 4, pp. 173–175, Apr. 2012.
- [6] P.-H. Deng, M.-I. Lai, S.-K. Jeng, and C. H. Chen, "Design of matching circuits for microstrip triplexers based on stepped-impedance resonators," *IEEE Trans. Microw. Theory Techn.*, vol. 54, no. 12, pp. 4185–4192, Dec. 2006.
- [7] X. Jin and Z. Yan, "Microstrip triplexer and switchable triplexer using new impedance matching circuits," *Int. J. RF Microw. Comput.-Aided Eng.*, vol. 27, no. 1, 2016, Art. no. e21057.
- [8] C. W. Tang and M. G. Chen, "Packaged microstrip triplexer with star-junction topology," *Electron. Lett.*, vol. 48, no. 12, pp. 699–701, Jun. 2012.
- [9] C. Zhu, J. Zhou, and Y. Wang, "Design of microstrip planar triplexer for multimode/multi-band wireless systems," *Microw. J.*, vol. 2010, pp. 1–19, Jan. 2010.
- [10] S.-C. Lin and C.-Y. Yeh, "Design of microstrip triplexer with high isolation based on parallel coupled-line filters using T-shaped short-circuited resonators," *IEEE Microw. Wireless Compon. Lett.*, vol. 25, no. 10, pp. 648–650, Oct. 2015.
- [11] A. El-Tokhy, R. Wu, and Y. Wang, "Microstrip triplexer using a common triple-mode resonator," *Microw. Opt. Technol. Lett.*, vol. 60, no. 7, pp. 1815–1820, Jul. 2018.
- [12] C.-F. Chen, T.-M. Shen, T.-Y. Huang, and R.-B. Wu, "Design of multimode net-type resonators and their applications to filters and multiplexers," *IEEE Trans. Microw. Theory Techn.*, vol. 59, no. 4, pp. 848–856, Apr. 2011.
- [13] A. Rezaei and L. Noori, "Novel low-loss microstrip triplexer using coupled lines and step impedance cells for 4G and WiMAX applications," *TURKISH J. Electr. Eng. Comput. Sci.*, vol. 26, no. 4, pp. 1871–1880, Jul. 2018.
- [14] S. Keshavarz, A. Abdipour, A. Mohammadi, and R. Keshavarz, "Design and implementation of low loss and compact microstrip triplexer using CSRR loaded coupled lines," *AEU-Int. J. Electron. Commun.*, vol. 111, Nov. 2019, Art. no. 152913.
- [15] A. Ching, A. Errkik, L. E. Abdellaoui, A. Tajmouati, J. Zbitou, and M. Latrach, "Design of a microstrip diplexer and triplexer using open loop resonators," *J. Microw., Optoelectron. Electromagn. Appl.*, vol. 15, no. 2, pp. 65–80, Jun. 2016.
- [16] H.-W. Wu, S.-H. Huang, and Y.-F. Chen, "Compact microstrip triplexer based on coupled stepped impedance resonators," in *IEEE MTT-S Int. Microw. Symp. Dig.*, Seattle, WA, USA, Jun. 2013, pp. 1–3.
- [17] T. Yang, P.-L. Chi, and T. Itoh, "Compact quarter-wave resonator and its applications to miniaturized diplexer and triplexer," *IEEE Trans. Microw. Theory Techn.*, vol. 59, no. 2, pp. 260–269, Feb. 2011.
- [18] T. Yang and G. M. Rebeiz, "A 1.26–3.3 GHz tunable triplexer with compact size and constant bandwidth," *IEEE Microw. Wireless Compon. Lett.*, vol. 26, no. 10, pp. 786–788, Oct. 2016.
- [19] J.-F. Qian and F.-C. Chen, "Wide stopband microstrip triplexer using common crossed, resonator and uniform impedance resonator," *Prog. Electromagn. Res. Lett.*, vol. 69, pp. 79–86, 2017.
- [20] A. Rezaei, S. I. Yahya, L. Noori, and M. H. Jamaluddin, "Design and fabrication of a compact microstrip triplexer for WiMAX and wireless applications," *Eng. Rev.*, vol. 41, no. 1, pp. 85–91, 2020.
- [21] T. Sugchai, I. Nattapong, and C. Apirun, "Design of microstrip triplexer using common dual-mode resonator with multi-spurious mode suppression for multiband applications," *Appl. Mech. Mater.*, vol. 763, pp. 182–188, May 2015.
- [22] L. Zhou, Z. Long, Q. Feng, Q. Jin, and Y. Li, "Channel-continuous triplexer with multiple transmission zeros based on cascaded high-pass and low-pass filters," *IEEE Microw. Wireless Compon. Lett.*, vol. 32, no. 5, pp. 395–398, May 2022.
- [23] M. Jamshidi, S. I. Yahya, L. Nouri, H. Hashemi-Dezaki, A. Rezaei, and M. A. Chaudhary, "A super-efficient GSM triplexer for 5G-enabled IoT in sustainable smart grid edge computing and the metaverse," *Sensors*, vol. 23, no. 7, p. 3775, Apr. 2023.
- [24] J. S. Hong and M. J. Lancaster, *Microstrip Filters for RF/Microwave Applications*. Hoboken, NJ, USA: Wiley, 2001.
- [25] S. I. Yahya, A. Rezaei, and L. Nouri, "Compact wide stopband microstrip diplexer with flat channels for WiMAX and wireless applications," *IET Circuits, Devices Syst.*, vol. 14, no. 6, pp. 846–852, Sep. 2020.
- [26] S. I. Yahya and L. Nouri, "A low-loss four-channel microstrip diplexer for wideband multi-service wireless applications," *AEU-Int. J. Electron. Commun.*, vol. 133, May 2021, Art. no. 153670.
- [27] Y. Liu, "A tri-band bandpass filter realized using tri-mode T-shape branches," *Prog. Electromagn. Res.*, vol. 105, pp. 425–444, 2010.
- [28] A. Rezaei and L. Noori, "Compact low-loss microstrip diplexer using novel engraved semi-patch cells for GSM and WLAN applications," *AEU-Int. J. Electron. Commun.*, vol. 87, pp. 63–158, Apr. 2018.
- [29] G. Wibisono, T. Firmansyah, and T. Syafraditya, "Design of triple-band bandpass filter using cascade tri-section stepped impedance resonators," *J. ICT Res. Appl.*, vol. 10, no. 1, pp. 43–56, Oct. 2016.
- [30] L. Noori and A. Rezaei, "Design of a microstrip diplexer with a novel structure for WiMAX and wireless applications," *AEU-Int. J. Electron. Commun.*, vol. 77, pp. 18–22, Jul. 2017.
- [31] F.-C. Chen, J.-M. Qiu, H.-T. Hu, Q.-X. Chu, and M. J. Lancaster, "Design of microstrip lowpass-bandpass triplexer with high isolation," *IEEE Microw. Wireless Compon. Lett.*, vol. 25, no. 12, pp. 805–807, Dec. 2015.
- [32] M. Karlsson, P. Hakansson, and S. Gong, "A frequency triplexer for ultra-wideband systems utilizing combined broadside- and edge-coupled filters," *IEEE Trans. Adv. Packag.*, vol. 31, no. 4, pp. 794–801, Nov. 2008.



**SALAH I. YAHYA** (Senior Member, IEEE) received the B.Sc. degree in electrical engineering, the M.Sc. degree in electronics and communication engineering, and the Ph.D. degree in communication and microwave engineering. He joined the Department of Software Engineering, Koya University, in 2010, where he is currently a Full Professor. He is a Consultant Engineer and a Senior Member of USA and AMTA-USA. He has many published research articles in high quality journals and he presented many conference papers. His research interests include antenna design, numerical RF dosimetry, MW measurement, and MW components design. He has been a regular reviewer of the Electromagnetics Academy, Cambridge, USA, PIERS Journals publications, *Science and Engineering of Composite Materials Journal* and *International Journal of Applied Electromagnetics and Mechanics*, since 2009.



**FARID ZUBIR** (Member, IEEE) received the B.Eng. degree in electrical (majoring in telecommunication) and the M.Eng. degree in RF and microwave from Universiti Teknologi Malaysia (UTM), in 2008 and 2010, respectively, and the Ph.D. degree from the University of Birmingham, U.K., in 2016, for research into direct integration of power amplifiers with antennas in microwave transmitters. He is currently an Assistant Professor and a Research Fellow with the Department of Communication Engineering, School of Electrical Engineering, and the Wireless Communication Centre, UTM, respectively. He was an Honorary Postdoctoral Research Fellow with The University of British Columbia (UBCO), Okanagan, BC, Canada, from September 2019 to August 2021, where he was conducting research into highly efficient and linear amplification power amplifier topology for wireless power systems. His research interests include the area of RF and microwave technologies, including linearization and high-efficiency techniques for PAs, beamforming networks, planar array antenna, dielectric resonator antenna (DRA), and active integrated antenna (AIA).



**LEILA NOURI** received the B.Sc. and M.Sc. degrees in electronic engineering from Razi University, Kermanshah, Iran, in 2005 and 2009, respectively, and the Ph.D. degree in electronic engineering from the Shiraz University of Technology. She is the author of one books, more than 60 articles, and more than five research and industrial projects. Her research interests include microstrip coupler, microstrip filter, neural networks, and LNAs.

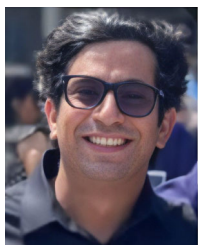


**MAHER ASSAAD** received the master's degree in electrical engineering/microelectronics IC design from the University of Montreal, Montreal, Canada, in 2002, and the Ph.D. degree in electrical engineering/microelectronics IC design from the University of Glasgow, Glasgow, U.K., in 2009. He was a Senior Lecturer of electrical engineering with the University Technology of PETRONAS, Malaysia, and an Associate Professor of electronic and communication engineering with the American University of Ras Al Khaimah, UAE. He is currently a Professor of electrical and computer engineering with Ajman University, United Arab Emirates. His research interests include the design of circuits/integrated circuits for various type of sensors and for wireline and optical communication systems.



circuits and computational intelligence.

**ABBAS REZAEI** was born in Kermanshah, Iran, in 1982. He received the B.S.E., M.S.E., and Ph.D. degrees in electronics engineering from Razi University, Kermanshah, Iran, in 2005, 2009, and 2013, respectively. He is currently an Associate Professor of electrical engineering with the Kermanshah University of Technology. He is the author of two books, more than 100 articles, and more than 10 research and industrial projects. His research interests include RF and microwave



include the characterization and fabrication of nanomaterials for the production of nanoscale electronic applications and electronic sensors of the next generation.

**FAWWAZ HAZZAZI** was born in Al-Kharj, Saudi Arabia. He received the B.S. degree in electrical engineering from the College of Engineering, Prince Sattam bin Abdulaziz University, Al-Kharj, the M.S. degree in electrical and computer engineering from The University of Maine, Orono, ME, USA, and the Ph.D. degree in electrical engineering from Louisiana State University, Baton Rouge, LA, USA. He has both industry and academic experience. His research interests



she joined Multimedia University, in 2004. She has presented technical papers at conference nationally and internationally. One of her conference papers has received the "Honorable Mention" for the Student Paper Competition from the International Microwave Symposium, USA, in 2011. She has authored/coauthored more than 50 journals and conference papers. Her teaching and research focus in the area of power amplifier design, antenna, 5G communications, and analog/mixed signal RF circuit design.

**ZUBAIDA YUSOFF** (Senior Member, IEEE) received the B.Sc. degree (cum laude) in electrical and computer engineering and the M.Sc. degree in electrical engineering from The Ohio State University, USA, in 2000 and 2002, respectively, and the Ph.D. degree from Cardiff University, Wales, U.K., in 2012. She holds the position of a Senior Lecturer with the Faculty of Engineering, Multimedia University. She was with Telekom Malaysia International Network Operation, in 2002, before



for High-Frequency Engineering, Cardiff University. He is currently an Associate Professor of electrical engineering with Ajman University. He is a Chartered Engineer of the Engineering Council, U.K., and a fellow of the Higher Education Academy, U.K. His research interests include nonlinear device characterization, spectrum-efficient power amplifiers, nonlinear measurement techniques, and microwave electronics have resulted in more than 100 academic articles.

**MUHAMMAD AKMAL CHAUDHARY** (Senior Member, IEEE) received the master's and Ph.D. degrees in electrical and electronic engineering from Cardiff University, Cardiff, U.K., in 2007 and 2011, respectively, and the MBA degree in leadership and corporate governance from the Edinburgh Business School, Heriot-Watt University, Edinburgh, U.K., in 2022. Before joining Ajman University, United Arab Emirates, in 2012, he held a Postdoctoral Research position with the Centre



innovation in engineering. Her research interests include the applications of artificial intelligence in engineering and exploring sustainable solutions in the field of engineering.

**BINH NGUYEN LE** received the B.Sc. and M.Sc. degrees in engineering from the Da Nang University of Technology, in 2011 and 2016, respectively. She is currently pursuing the Ph.D. degree in engineering, further expanding her knowledge and expertise in the field. She is a dedicated Researcher and an Academician in the field of engineering. As a member of the Research and Development Institute, Duy Tan University, she actively contributes to the advancement of knowledge and